Type 2 Deiodinase Disruption in Astrocytes Results in Anxiety-Depressive-Like Behavior in Male Mice

Barbara M. L. C. Bocco, João Pedro Werneck-de-Castro, Kelen C. Oliveira, Gustavo W. Fernandes, Tatiana L. Fonseca, Bruna P. P. Nascimento, Elizabeth A. McAninch, Esther Ricci, Zsuzsanna Kvárta-Papp, Csaba Fekete, Maria Martha Bernardi, Balázs Gereben, Antonio C. Bianco, and Miriam O. Ribeiro*

Millions of levothyroxine-treated hypothyroid patients complain of impaired cognition despite normal TSH serum levels. This could reflect abnormalities in the type 2 deiodinase (D2)-mediated T_4-to-T_3 conversion, given their much greater dependence on the D2 pathway for T_3 production. T_3 normally reaches the brain directly from the circulation or is produced locally by D2 in astrocytes. Here we report that mice with astrocyte-specific *Dio2* inactivation (Astro-D2KO) have normal serum T_3 but exhibit anxiety-depression-like behavior as found in open field and elevated plus maze studies and when tested for depression using the tail-suspension and the forced-swimming tests. Remarkably, 4 weeks of daily treadmill exercise sessions eliminated this phenotype. Microarray gene expression profiling of the Astro-D2KO hippocampi identified an enrichment of three gene sets related to inflammation and impoverishment of three gene sets related to mitochondrial function and response to oxidative stress. Despite normal neurogenesis, the Astro-D2KO hippocampi exhibited decreased expression of four of six known to be positively regulated genes by T_3, ie, *Mbp* (~43%), *Mag* (~34%), *Hr* (~49%), and *Aldh1a1* (~61%) and increased expression of 3 of 12 genes negatively regulated by T_3, ie, *Dgkg* (~17%), *Syce2* (~26%), and *Col6a1* (~3-fold) by quantitative real-time PCR. Notably, in Astro-D2KO animals, there was also a reduction in mRNA levels of genes known to be affected in classical animal models of depression, ie, *Bdnf* (~18%), *Ntf3* (~43%), *Nmdar* (~26%), and *GR* (~20%), which were also normalized by daily exercise sessions. These findings suggest that defects in Dio2 expression in the brain could result in mood and behavioral disorders. (*Endocrinology* 157: 3682–3695, 2016)

Thyroid hormone molecules reach the brain through the circulation and within the brain undergo controlled metabolism that can either result in activation or terminal inactivation. The prohormone T_4 crosses the blood-brain barrier via specific transporters, eg, organic anion-transporting polypeptide (Oatp), and can then be taken up by glial cells via monocarboxylate transporters such as monocarboxylate transporter 10 (1). Inside the glial cells, T_4 is deiodinated to the active hormone T_3 by the type 2 deiodinase (D2), a small integral membrane dimeric protein with a selenocysteine-containing active center embed-

ded in a thioredoxin-like fold (2, 3). D2-generated T_3 normally diffuses from the glial cells into neighboring neurons via the monocarboxylate transporter 8 (Mct8), in which it acts in a paracrine fashion to modulate T_3-responsive genes (4).

Knowledge about thyroid hormone homeostasis in the brain was advanced by studies in which rats received timed injections of 125I-T_4 that was followed by quantification of 125I-T_3 bound to thyroid hormone receptor (TR) in whole brains. As opposed to most other tissues, there is a high degree of occupancy of TRs in the rat brain, almost

saturation, with predominant contribution by locally D2-produced T_3 (5, 6). Direct quantification of T_3 in the brain revealed that the cerebellum, hypothalamus, and midbrain of a mouse with global inactivation of the *Dio2* gene (global-D2KO) contain less T_3, depending on the age of the animal (7, 8). Subsequent studies reported that the expression of only one (of 18) T_3 positively regulated genes was decreased in the cerebral cortex of 21-day-old global-D2KO mice and that the expression of 12 (of the 15) T_3 negatively regulated genes was increased (9). Similar results were obtained in 21- and 50-day-old global-D1/D2KO animals (10).

Neurons express the inactivating type 3 deiodinase (D3), which inactivates both T_4 and T_3 and has been shown to dampen thyroid hormone signaling in a cell- or tissue-specific fashion (4). In neurons D3 is located in the plasma membrane and in the membranes of dense core vesicles (11, 12). However, D3 can accumulate in the nuclear membrane under ischemic and/or hypoxic conditions, in which it dampens thyroid hormone signaling (4, 13). In addition, there is elevated T_3 content in the brains of mice with inactivation of the *Dio3* gene (D3KO) (14).

Therefore, thyroid hormone signaling in the brain depends on plasma T_4 and T_3, membrane transporters, and the expression of D2 and D3, which provides a means to localized control of thyroid hormone action. In addition, these two deiodinases also constitute a homeostatic advantage given their reciprocal response to hypothyroidism (15, 16): D2 activity accelerates and D3 activity slows down, increasing fractional conversion of T_4 to T_3 and decreasing T_4 and T_3 clearance rates (17). However, the lack of a significant neurological phenotype in the global-D2KO mouse has placed in check the relevance of the D2 pathway and the local T_3 production in the brain (7). After extensive neurological testing of the global-D2KO mouse, including reflexes, olfaction, coordination of motor systems, learning and memory, and anxiety, the only finding was diminished agility (7). These minimal findings could also reflect successful activation of homeostatic processes that compensate for the lack of T_3 production in the brain. In the present study, we sought to obtain new insight into the role played by D2 pathway in the brain by phenotypically characterizing mice that have selective inactivation of *Dio2* in astrocytes (Astro-D2KO). These animals are systemically euthyroid and have normal serum thyroid hormone levels (18) but do exhibit accelerated diurnal rate of fatty acid oxidation (19).

Materials and Methods

All experiments were planned according to the American Thyroid Association guide to investigating thyroid hormone economy and action in rodent and cell models (20) and were approved by the Institutional Animal Care and Use Committee at Rush University Medical Center.

Animals

Astro-D2KO mice were created and maintained as described previously (18). Briefly, floxed D2 mice (Dio2^{Flx}) (87.5% B6, 12.5% 129sv) were crossed with transgenic mice expressing Cre recombinase under the glial fibrillary acidic protein promoter (GFAP-Cre; FVB-Tg[GFAPCre]25Mes/J; The Jackson Laboratory) backcrossed seven times with B6 mice. GFAP-Cre littermate animals were used as controls throughout the studies. In all experiments, 9- to 14-week-old male mice housed in standard plastic cages (four per cage) were kept at room temperature (22°C), with a 12-hour dark, 12-hour light cycle starting at 6:00 AM. Animals were kept on standard chow diet (3.1 kcal/g; 2918 Teklad Global Protein Rodent Diet; Harlan Laboratories). All animals were killed by asphyxiation in a CO_2 chamber or by transcardiac perfusion with fixative solution after anesthesia.

Comprehensive lab animal monitoring system (CLAMS)

Ambulatory activity profiles were obtained by admitting mice to individual cages with free access to food and water for 1 week in a CLAMS (Columbus Instruments). This system allows for continuous measurement of movement inside the cage: X (front to back), Y (right to left), Z (rearing), and distance (centimeters); all studies were performed after a 48-hour adaptation period. In a separate study, animals were allowed to use the free-running wheel and data reported as accumulated revolutions per 48 hours.

Behavioral testing

With the exception of the open field test (7:00–9:00 AM), all behavioral tests were performed in the afternoon (3:00–5:00 PM), in the following order:

Open field test (OFT)

The OFT was used for the assessment of locomotor and exploratory activity (21). The apparatus was located in a 1.8- × 4.6-m test room with background lighting provided by a 15-lux lamp; the apparatus was washed with a 5% alcohol-water solution before placement of the animals. Animals were tested in an

Division of Endocrinology and Metabolism (B.M.L.C.B., J.P.W.-d.C., G.W.F., T.L.F., E.A.M., A.C.B.), Rush University Medical Center, Chicago, Illinois 60612; Department of Translational Medicine (B.M.L.C.B., G.W.F., B.P.P.N.), Federal University of Sao Paulo, Sao Paulo SP, 04039-002, Brazil; Biophysics Institute and School of Physical Education and Sports (J.P.W.-d.C.), Federal University of Rio de Janeiro, RJ 21941-599, Brazil; Department of Clinic Endocrinology (K.C.O.), Federal University of Sao Paulo, Sao Paulo SP 04039-032, Brazil; Developmental Disorders Program (B.P.P.N., E.R., M.O.R.), Center of Biological Science and Health, Mackenzie Presbyterian University, Sao Paulo SP 01302-900 Brazil; Department of Endocrine Neurobiology (Z.K.-P., C.F., B.G.), Institute of Experimental Medicine, Hungarian Academy of Sciences, Budapest H-1083, Hungary; Department of Medicine (C.F.), Division of Endocrinology, Diabetes, and Metabolism, Tupper Research Institute, Tufts Medical Center, Boston, Massachusetts 02111; and Graduate Program of Environmental and Experimental Pathology (M.M.B.), Graduate Program of Dentistry, Universidade Paulista, Sao Paulo SP 04026-002, Brazil

acrylic squared arena (72 × 72 cm) surrounded by a 30-cm wall. The floor of the arena was marked with lines delimitating sixteen 18- × 18 cm-squares; mice were placed into the center of the arena and observed for 5 minutes; all tests were recorded by video camera for later analysis of the following: 1) time in the open field center; 2) total entries in the open field center; 3) total number of lines crossed with four paws; 4) rearing; 5) freezing; and 6) grooming.

Elevated plus maze (EPM)

The EPM was made of plywood covered with plastic and consisted of two opposed open arms (30 × 5 cm) and two opposed enclosed arms (30 × 5 × 15 cm) connected by a central open square (5 × 5 cm) (21). The maze was elevated 38 cm above the floor and placed inside a room free of noise and disturbances, under laboratory dim light; the test was recorded by video camera for later analysis. Animals were placed into the central square of the maze facing one of the open arms and observed for 5 minutes for the following: 1) number of entries into open and enclosed arms; 2) time spent inside the open and enclosed arms; 3) rearing; 4) time of freezing; and 5) number of head dips (22).

Tail suspension test (TST)

The TST involves suspending a mouse by the tail and measurement of the immobility time. The mouse is suspended in the center of a container with width and depth sufficiently sized so that the mouse cannot make contact with the walls. In this setting, the approximate distance between the mouse's nose and the floor is 20–25 cm. A plastic suspension bar (1 cm height × 1 cm width × 60 cm length) used to suspend the tail is positioned on top of the box (21). Mice were suspended for 5 minutes and the test taped with a video camera for later analysis. Immobility was defined as the lack of movement of any limbs.

Forced swim test (FST)

The FST was performed in a cylindrical tank (30 cm height × 20 cm diameter) made of transparent Plexiglas (21). The water level was 15 cm from the bottom and was marked on the tank wall to ensure consistency throughout the studies. The dimensions of the tank were selected so that mice were not be able to touch the bottom of the tank, either feet or tail, during the test and tall enough to prevent the mice from escaping. Mice were place into the water (28°C-30°C) for two 5-minute sessions. Each animal underwent one test per day on 2 consecutive days. The tests were taped with a video camera for later analysis. Each animal was scored as either floating or swimming. Floating was defined as the lack of movement of any limbs. Before returning the animals to the home cages, they were dried gently and kept under a heat lamp to prevent hypothermia.

Treadmill exercise protocol

Mice were placed on the motorized treadmill (Columbus Instruments) following an exercise protocol consisting of 30 minutes of treadmill running at 13 m/min, five times a week for 4 weeks with no inclination. In separate experiments, animals underwent exercise training for 30 minutes once a day for 5 consecutive days at 60% of maximum speed (S_{max}). S_{max} was determined through the maximal exercise capacity test as previously described (23, 24). Mice were euthanized 3 hours after the last session of exercise. The brain was dissected, snap frozen, and stored in liquid nitrogen for further analysis. All exercise sessions were performed between 1:00 and 5:00 PM.

Brain regions dimensions

Sections mounted on gelatin-coated slides were dehydrated with ascending series of ethanol, treated with xylene for 5 minutes, and rehydrated in descending series of ethanol and in MilliQ water. Then the sections were treated with 1% cresyl violet (Sigma) solution for 3 minutes followed by differentiation in acetic acid in 100% ethanol (at 1:50 000 dilution) for 5 seconds. Then the sections were dehydrated in ascending series of ethanol, treated with xylene, and coverslipped using DPX mounting medium (Sigma-Aldrich, Inc). The ImageJ software (National Institutes of Health, Bethesda, Maryland) was used to perform the measurements on Nissl-stained sections (n = 6). The following parameters were measured and expressed in micrometers: hippocampus − total height and height of dentate gyrus; cerebellum − height of stratum granulosum; cerebral cortex − heights of layers 2–6.

Myelin basic protein (MBP) labeling in the hippocampus and corpus callosum

Mice were anesthetized with ketamine (100 mg/kg) and xylazine (5 mg/kg) ip and perfused transcardially with 10 mL PBS (pH 7.4) followed by 40 mL 4% paraformaldehyde in 0.1 M phosphate buffer (pH 7). Brains were removed and cryoprotected in 30% sucrose in PBS. The brains were frozen in powdered dry ice, and coronal, 25-μm-thick sections were prepared with a freezing microtome (Leica). The sections were collected in freezing solution (30% ethylene glycol; 25% glycerol; 0.05 M phosphate buffer) and stored at −20°C until used. The sections were washed three times in PBS and then in 0.5% Triton X-100 + 0.5% H_2O_2 in PBS 15 minutes and rinsed again in PBS three times. The nonspecific antibody binding was blocked by treatment in 2% normal horse serum in PBS for 20 minutes followed by incubation in rabbit anti-MBP primary antibody (1:250, AB980; Merck-Millipore) for 24 hours and washed in PBS. Fluorescein -conjugated anti-rabbit IgG (1:250; Jackson ImmunoResearch) was applied for 1.5 hours and the sections were washed again in PBS three times. The sections were mounted on glass slides and coverslipped with Vectashield mounting medium (Vector). The ImageJ software (National Institutes of Health) was used to measure total density of the whole hippocampus (n = 6).

Examination of the adult neurogenesis

Injection of 5-bromo-2′-deoxyuridine (BrdU; 80 mg/kg; sc; Sigma-Aldrich) was performed for 2 consecutive days, five times per day in 8 hours. Subsequently, animals were anesthetized and perfused with fixative and 25-μm-thick coronal brain sections were prepared as described above. The sections were also pretreated based on the above-described protocol. To label the perikarya of neurons, the sections were incubated in mouse anti-HuC/D biotinylated antibody (1:300; Life Technologies) for 2 days at 4°C. After washing in PBS, the sections were immersed in avidin-biotin complex (1:1000, ABC Elite kit; Vector) for 1 hour, followed by rinses in PBS. Sections were subjected to biotinylated tyramide amplification using the tyramide signal amplification kit according to the manufacturer's instructions (NEN Life Science Products) and then washed in PBS three times.

This was followed by incubation in 2 M HCl for 2 hours and then washed in PBS four times. Section were incubated with fluorescein-conjugated streptavidin (1:250; Vector) for 1.5 hours and washed in PBS three times. This was followed by incubation in sheep anti-BrdU antibody (1:300; Abcam) for 24 hours, washed in PBS three times, and then incubated with Alexa-555-conjugated antisheep IgG (1:250; Life Technologies) and washed in PBS three times. Sections were mounted on glass slides and coverslipped with Vectashield mounting medium (Vector).

Deiodinase assays

D2 and D3 assays were performed in sonicates of brain and pituitary gland tissue in the presence of 10 mM ditiotreitol and 0.25 M sucrose as described previously (20). D2 assays were performed using 1 nM 125I-(5′) T_4 (PerkinElmer) in the presence of 1 mM propylthiouracil and 10 nM T_3 to minimize T_4 deiodination by D3 (20). D3 activity was measured as previously described in the presence of 0.2 nM 125I-(5′) T_3 (PerkinElmer). Reactions were stopped by the addition of methanol, and the products of deiodination were quantified by ultraperformance liquid chromatography (ACQUITY; Waters Corp.). Fractions were automatically processed through a Flow Scintillation Analyzer Radiomatic 610TR (PerkinElmer) for radiometry.

Gene expression analysis

Total tissue RNA was extracted from the hippocampus and cerebral cortex using the RNeasy lipid tissue minikit (QIAGEN), following the manufacturer's instructions including deoxyribonuclease treatment for 30 minutes. RNA was quantified with a NanoDrop spectrophotometer, and 0.5–1.0 μg total RNA was used to produce cDNA using the Transcriptor first-strand cDNA synthesis kit (Roche). Quantitative real-time PCR (RT-qPCR) conditions were performed as previously described (25). We used either primers designed to span exon-exon and/or intron-spanning sequences or previously validated (https://pga.mgh.harvard.edu/primerbank/). All primer sequences are listed in Supplemental Table 1. Genes of interest were analyzed (StepOne; Applied Biosystems) using PerfeCTa SYBR Green Fastmix Rox (Quantas). The melting curve protocol was used to verify the specificity of the amplicon generation. Standard curves consisted of four to five points of serially diluted mixed experimental and control group cDNA. Cyclophilin A (CycloA) was used as a housekeeping internal control gene; its expression level was similar between groups. The coefficient of correlation was greater than 0.99 for all curves, and the amplification efficiency ranged between 80% and 110%. Results were expressed as the ratio of test mRNA to CycloA mRNA.

The following genes were studied: iodothyronine deiodinase, type II (*Dio2*), monocarboxylate transporter 8 (*Mct8*), organic anion-transporting polypeptide 14 (*Oatp14*), myelin basic protein (*Mbp*), myelin-associated glycoprotein (*Mag*), hairless (*Hr*), aldehyde dehydrogenase family 1, subfamily A1 (*Aldh1a1*), RNA binding motif protein 3 (*Rbm3*), neurogranin (*Nrgn*), 3-hydroxy-3-methylglutaryl-coenzyme A synthase 2 (*Hmgsc2*), hyaluronan and proteoglycan link protein 1 (*Hapln1*), diacylglycerol kinase, γ (*Dgkg*), cold inducible RNA binding protein (*Cirbp*), icos ligand (*Icosl*), MARCKS-like 1 (*Marcksl1*), solute carrier family 1 (glial high affinity glutamate transporter), member 3 (*Slc1a3*), outer dense fiber of sperm tails 4 (*Odf4*), synaptonemal complex central element protein 2 (*Syce2*), collagen,

type VI, α1 (*Col6a1*), sulfotransferase family 1A, phenol-preferring, member 1 (*Sult1a1*), ATP/GTP binding protein-like 3 (*Agbl3*), 5-hydroxytryptamine (serotonin) receptor 1A (*Htr1a*), 5-hydroxytryptamine (serotonin) receptor 1B (*Htr1b*), brain-derived neurotrophic factor (*Bdnf*), neurotrophin 3 (*Ntf3*), ciliary neurotrophic factor (*Cntf*), nerve growth factor (*Ngf*), vascular endothelial growth factor a (*Vegfa*), glutamate receptor, ionotropic, N-methyl-D-aspartate 1 (*Nmdar*), neuronal PAS domain protein 4 (*Npas4*), Nuclear receptor subfamily 3, group C, member 1 (*GR*).

Microarray

Hippocampi from four control and four Astro-D2KO mice were dissected as above and RNA prepared using the RNeasy lipid tissue minikit (QIAGEN) as per the manufacturer's instructions. Microarray analysis was performed by the Joslin Diabetes Center Genomics Core Laboratory (Boston, Massachusetts). Gene expression was evaluated using Genechip Mouse Gene 2.0 ST arrays (Affymetrix, Inc) that uses a whole-genome design to assess more than 35 000 transcripts. Gene expression data were preprocessed using Affymetrix Expression Console. Differential expression analysis was performed in Affymetrix transcriptome analysis console to identify individual genes demonstrating enrichment in the comparison of control vs Astro-D2KO animals. Expression values (signal) of individual genes were $\log_2$ transformed. One-way ANOVA was used to calculate the *P* values for each fold change (linear); multitesting correction was then performed using the Benjamini-Hochberg Step-Up false discovery rate (FDR)-controlling procedure for all the expressed genes. Individual genes demonstrating differential expression were considered statistically significant with an ANOVA *P* < .05; gene ontology analysis was used to determine the differences in gene sets between control and Astro-D2KO animals (Gene Set Enrichment Analysis [GSEA]; Broad Institute, Cambridge, Massachusetts). Expression values for all genes from all eight samples were used; no filter was applied to eliminate genes with low expression. GSEA included calculation of enrichment scores, estimation of significance level of enrichment scores (nominal *P* value), and adjustment for multiple hypothesis testing including the normalized enrichment score and FDR. There were no gene sets with an FDR of 25% or less, so a nominal value of *P* < 1% was chosen to indicate significance.

Statistical analyses

Data are expressed as mean ± SEM and were analyzed using PRISM software (GraphPad Software). A one-way ANOVA was used to compare more than two groups, followed by the Student-Newman-Keul's test to detect differences between groups. The Student's *t* test was used when only two groups were part of the experiment; *P* < .05 was used to reject the null hypothesis.

Results

Structural analysis and deiodinase expression in the Astro-D2KO brain

No differences in D2 activity were observed in cerebral cortex, hippocampus, or cerebellum of Dio2^{flx} or GFAP-Cre mice when compared with wild-type animals (Sup-

plemental Figure 1A–C). Astro-D2KO animals exhibited 70%–95% reduction in *Dio2* mRNA levels and D2 activity in the cerebral cortex and hippocampus (Figure 1, A–D) when compared with GFAP-Cre (control) animals. D2 activity was preserved in the pituitary gland (Figure 1E) and hypothalamus (18); D3 activity in hippocampus was unchanged in the Astro-D2KO animals (Figure 1F). No differences in the thyroid hormone transporters *Mct8*

and *Oatp14* mRNA levels in hippocampus or cerebral cortex were observed (Figure 1, G and H, and Supplemental Figure 1, D and E).

The dimensions of the hippocampus (Figure 1, I, P, and S), dentate gyrus (Figure 1, J, P, and S), cerebellum (Figure 1, K, Q, and T), and cerebral cortex (Figure 1, L, R, and U) were similar in Astro-D2KO and control animals. In addition, the number of BrdU-HuC/D-positive newborn
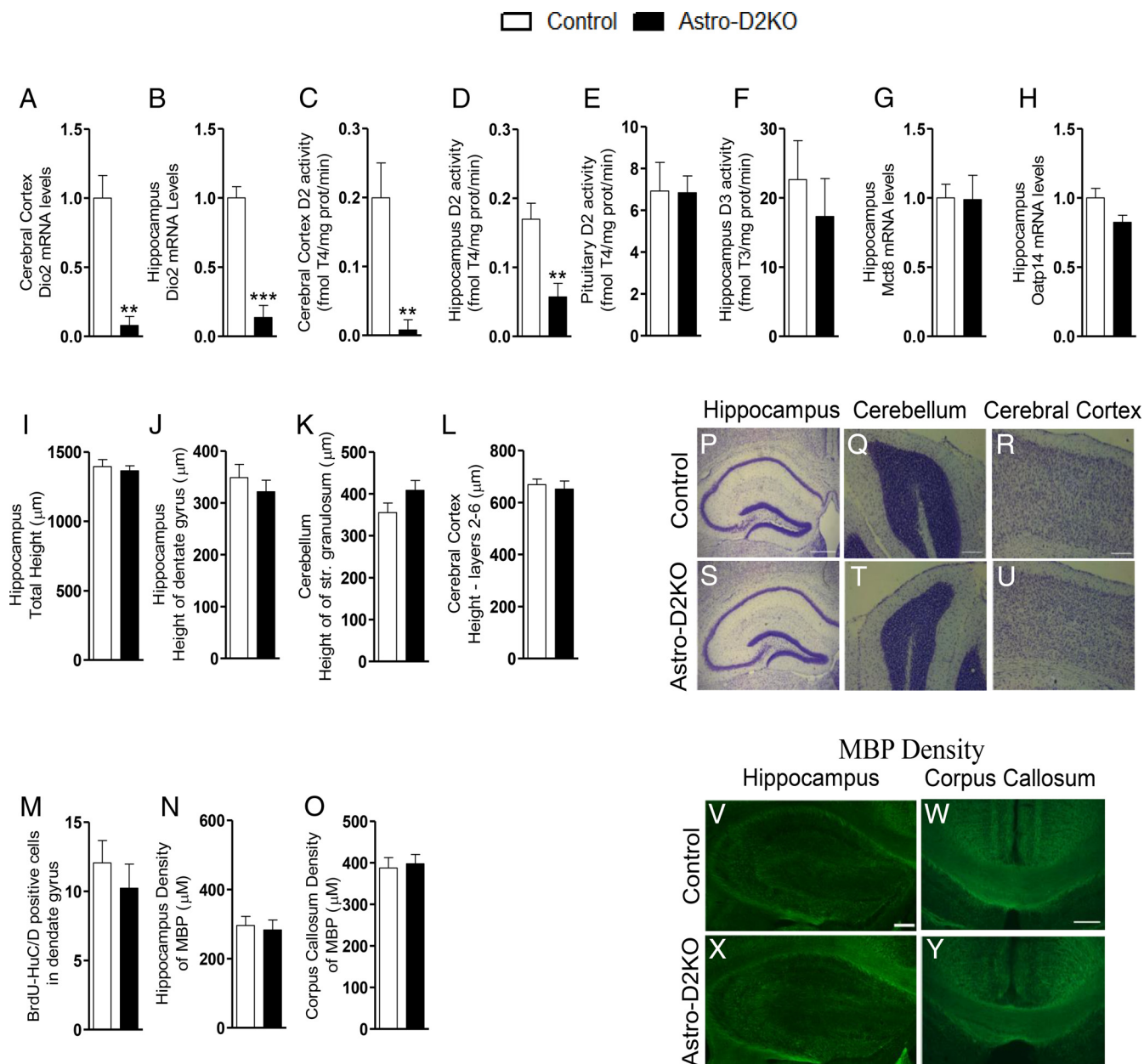
Figure 1. Deiodinases, gene expression, and histological structure in Astro-D2KO Brain. A and B, *Dio2* mRNA levels in cerebral cortex and hippocampus. C–E, D2 activity in the cerebral cortex, hippocampus, and pituitary gland. F, D3 activity in the hippocampus. G and H, *Mct8* and *Oatp14* mRNA levels in the hippocampus. Nissl-stained sections: I, hippocampus, total height (μM); J, hippocampus, height of dentate gyrus (μM); K, cerebellum, height of str. granulosum (μM); and L, cerebral cortex, heights of layers 2–6 (μM). M, Number of BrdU-HuC/D-positive cells in dentate gyrus. Density of MBP: N, hippocampus (μM); and O, corpus callosum (μM). Low-power magnification images illustrating Nissl-stained sections: P–S, hippocampus (HC), Q–T, cerebellum (CB), and R–U, cerebral cortex of control and Astro-D2KO animals. Nissl hippocampus, 500 μM; Nissl stained cerebral cortex and cerebellum, 200 μM. Low-power magnification immunofluorescence images illustrating MBP expression: V–X, hippocampus and W–Y, corpus callosum in control and Astro-D2KO animals. Fluor hippocampus and corpus callosum, 200 μM. Values are the mean $\pm$ SEM (n = 5–8). **, $P < .01$, ***, $P < .001$ as compared with control mice.

neurons in dentate gyrus (Figure 1M) and the density of MBP in the hippocampus (Figure 1, N, V, and X) and corpus callosum (Figure 1, O, W, and Y), as assessed by immunohistochemistry, was not affected as well.

The Astro-D2KO mouse exhibits anxiety-depression-like behavior

Astro-D2KO animals were housed for 7 days in rectangular cages and monitored continuously for ambulatory activity. Ambulatory activity toward the side of the cage containing food/water (x-axis) was similar in both control and Astro-D2KO animals (Figure 2, A–D). However, Astro-D2KO animals exhibited 23%–27% reduction in ambulatory activity during the light and dark periods in other areas of the cage (y-axis; Figure 2, E–H) as well as about 35% reduction in rearing during the dark period (Z-axis; Figure 2, I–L). The analyses of the combined ambulatory activity (x- plus y-axes) indicate that

Astro-D2KO animals exhibit less overall activity both in the light and dark segments of the cycle, although this difference was only borderline statistically significant (Supplemental Figure 2, A–C; $P = .07$). At the same time, when light and day segments were combined, Astro-D2KO animals exhibited about 16% decreased ambulatory activity (Supplemental Figure 2D). The physical distance covered within the first 12 hours of being moved into the cage (Figure 2M) as well as during the whole 7-day period of observation was about 18% less in the Astro-D2KO animals (Figure 2N). In a separate experiment, all animals were allowed to use the free-running wheel for 48 hours. There were no differences between control and Astro-D2KO animals when the accumulated total number of revolutions was compared (Supplemental Figure 3A).

The selective reduction in ambulatory activity potentially indicates the presence of mood disorders, which was
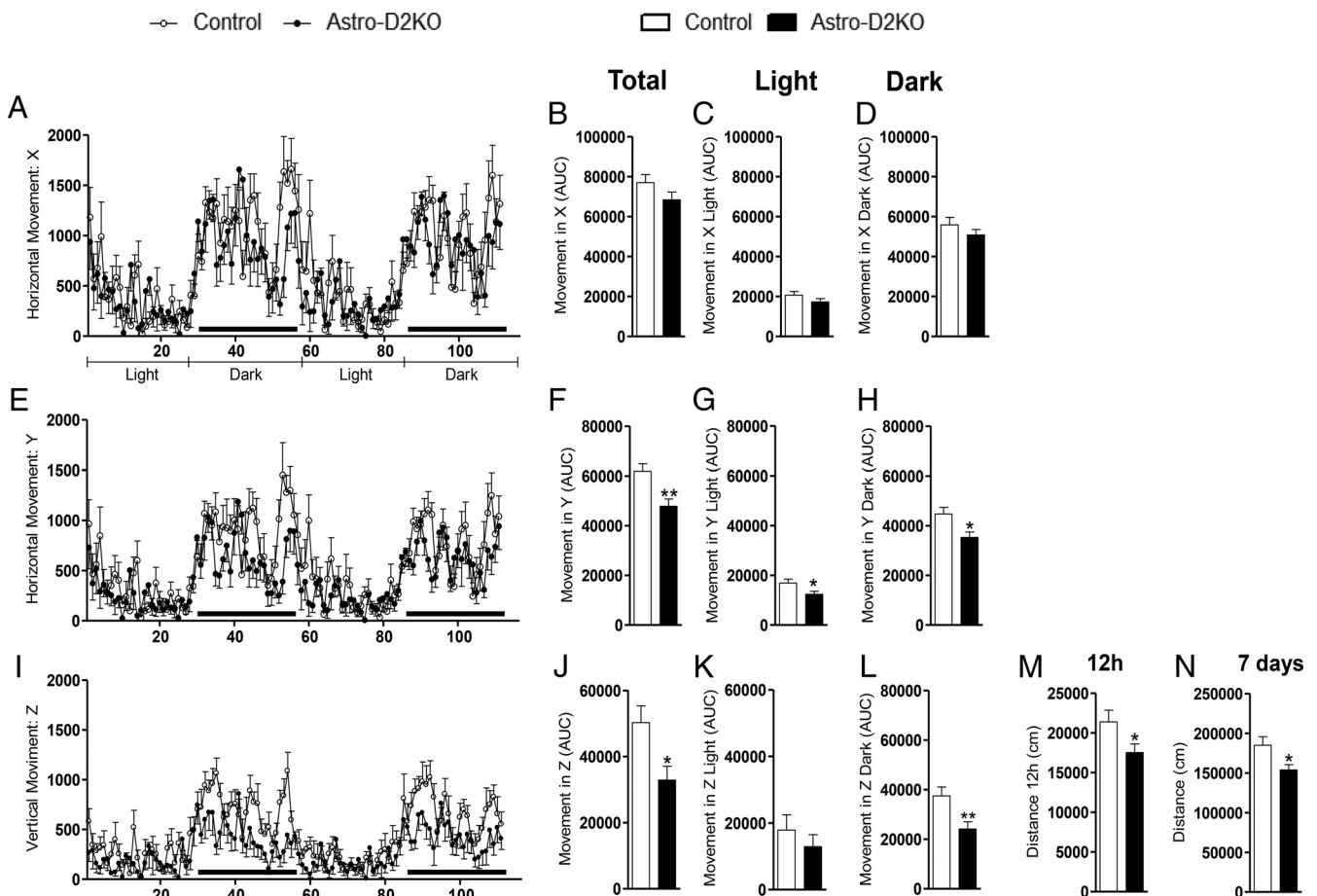
Figure 2. Forty-eight-hour locomotion profile in Astro-D2KO mice. A, Horizontal movement (X) registered for 48 hours during light and dark cycles. B, Area under the curve (AUC) of total X. C, AUC of X during light cycle. D, AUC of X during dark cycle. E, Same as in panel A, except that what is shown is horizontal movement (Y). F, Same as in panel B, except that what is shown is Y. G, Same as in panel C, except that what is shown is Y. H, Same as in panel D, except that what is shown is horizontal movement (Y). I, Same as in panel A, except that what is shown is vertical movement (Z). J, Same as in panel B, except that what is shown is vertical movement (Z). K, Same as in panel C, except that what is shown is vertical movement (Z). L, Same as in panel D, except that what is shown is vertical movement (Z). M, Traveled distance during the initial 12 hours in CLAMS. N, Traveled distance during 7 days in CLAMS. Values are the mean ± SEM (n = 12–13). *, $P < .05$, **, $P < .01$ compared with control mice.

subsequently tested in a series of behavioral studies. Astro-D2KO mice were first exposed to the open field under conditions of low light intensity, which sets a low emotionality context. The Astro-D2KO animals exhibited an approximately 1.8-fold increase in the number of center entries (Figure 3A) and an approximately 1.3-fold increase in rearing activity (Figure 3B), but no differences in exploratory activity (Figure 3C), time spent in the center field (Figure 3D), freezing (Figure 3E), or grooming (Figure 3F) were detected.

Next, animals were studied in the EPM to assess anxiety. No differences were observed on the time spent in the open arms (Figure 3G), in rearing behavior (Figure 3H), or the number of open arms entries (Supplemental Figure 2E). However, Astro-D2KO animals spent about 15% more time inside the closed arms (Figure 3I), almost doubled the time of freezing behavior (Figure 3J), exhibited approximately 42% less head dipping (Figure 3K), and

32% fewer entries in the closed arms (Supplemental Figure 2F), all results compatible with anxiety. Animals were then tested for depression using the tail-suspension and the forced-swimming tests. The Astro-D2KO animals exhibited 37%–42% more immobility time during both tests (Figure 3, L and M).

Astro-D2KO hippocampus exhibits a distinct transcriptome

An unbiased approach to gene expression in the hippocampus with microarray analysis was used to study changes resulting from astrocyte-specific *Dio2* inactivation. Differential expression analysis was used to identify individual genes with significantly different expression between control and Astro-D2KO animals. At a fold change $\geq$ 1.3 and $P < .05$, 30 named genes were down-regulated in Astro-D2KO and 43 up-regulated in the Astro-D2KOs (Tables 1 and 2).
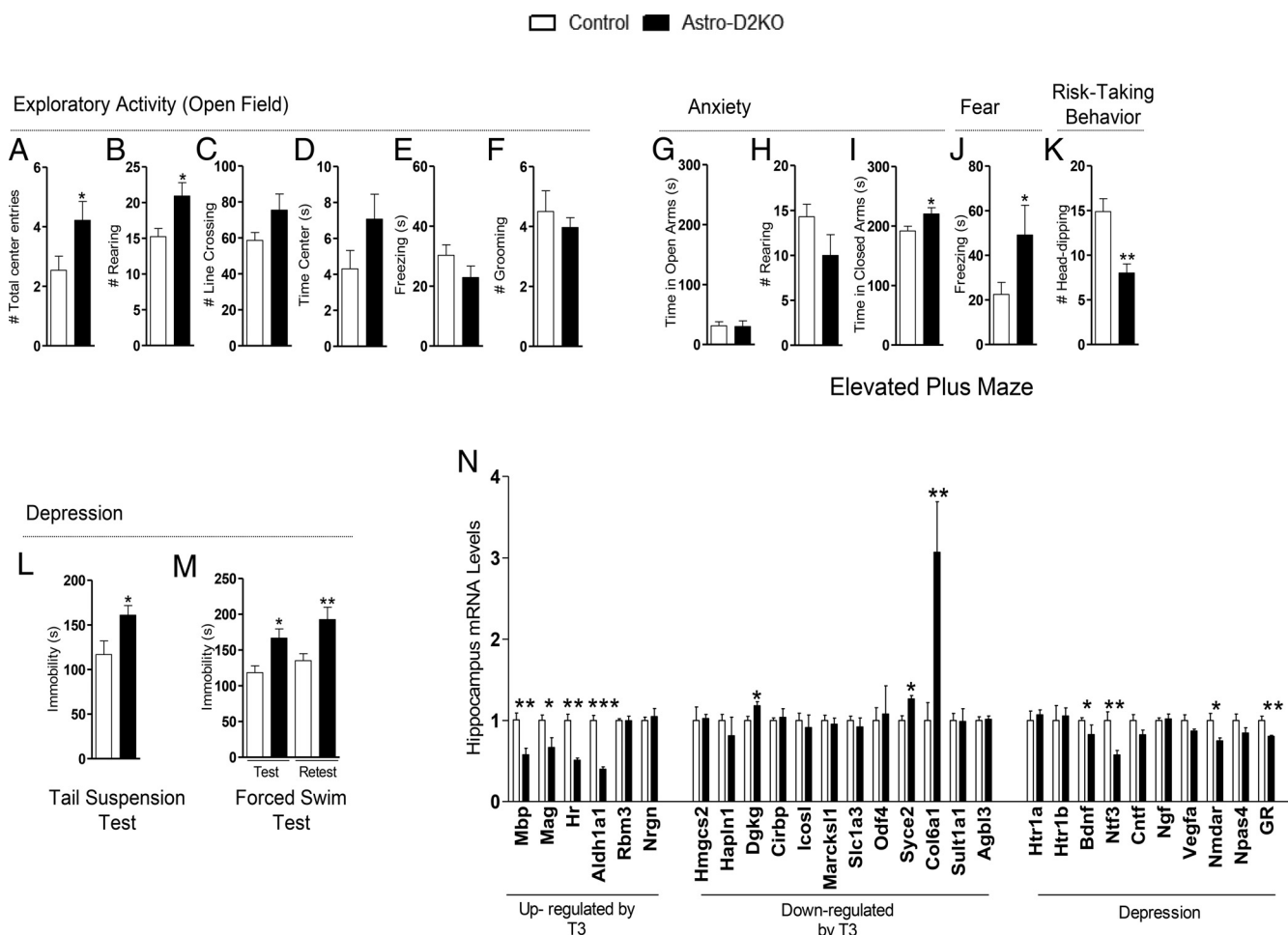
Figure 3. Behavior phenotype and hippocampal gene profile in Astro-D2KO mice. A–M, Behavioral tests. A–F, OFT. A, Total number of center entries. B, Total number of rearing. C, Total number of line crossing. D, Total time in center. E, Total time of freezing. F, Total number of grooming. G–K, EPM. G, Time spent in open arms. H, Total number of rearing. I, Time spent in closed arms. J, Total time of freezing. K, Total number of head dips. L, TST, time of immobility. M, FST, time of immobility. N, Gene profile in hippocampus. mRNA levels of T$_3$-responsive genes and genes related to depression, measured by RT-qPCR and using CycloA as the internal control. Values are the mean $\pm$ SEM (n = 8–17). *, $P <$ .05, **, $P <$ .01, ***, $P <$ .001 compared with control mice.

Table 1. Individual Gene Transcripts Down-Regulated in Astro-D2KO Hippocampus

Gene Symbol	Description	Fold	P Value
Dio2	Deiodinase, iodothyronine, type II	2.78	.000 099
Snord42a	Small nucleolar RNA, C/D box 42A	1.82	.036 107
Snord61	Small nucleolar RNA, C/D box 61	1.54	.005 067
Mir1224	microRNA 1224; von Willebrand factor A domain containing 5B2	1.49	.033 586
Cyp1b1	Cytochrome P450, family 1, subfamily b, polypeptide 1	1.46	.033 156
Olfr344	Olfactory receptor 344	1.46	.035 988
Snord110	Small nucleolar RNA, C/D box 110	1.46	.013 684
Lum	Lumican	1.45	.027 892
Ighv10−1	Ig heavy variable 10-1	1.41	.021 021
Snord69	Small nucleolar RNA, C/D box 69	1.41	.013 871
Mir5127	microRNA 5127	1.41	.039 012
Snord49b	Small nucleolar RNA, C/D box 49B	1.38	.026 267
Ddit4	DNA-damage-inducible transcript 4	1.37	.010 851
Ighj2	Ig heavy joining 2	1.37	.030 082
Snord55	Small nucleolar RNA, C/D box 55	1.37	.030 719
Cyp2j6	Cytochrome P450, family 2, subfamily j, polypeptide 6	1.36	.024 732
Ankrd34c	Ankyrin repeat domain 34C	1.36	.023 905
Phlda2	Pleckstrin homology-like domain, family A, member 2	1.35	.03 254
Rhox3f	Reproductive homeobox 3F	1.34	.017 248
Vmn1r120	Vomeronasal 1 receptor 120	1.33	.025 518
Phf1	PHD finger protein 1	1.32	.047 541
Myom1	Myomesin 1	1.32	.004 866
Snord16a	Small nucleolar RNA, C/D box 16A	1.32	.011 198
Snord49a	Small nucleolar RNA, C/D box 49A	1.31	.045 041
Cyth3	Cytohesin 3	1.31	.031 086
Tuba3a	Tubulin, α3A; tubulin, α3B	1.31	.044 086
Mageb1	Melanoma antigen, family B, 1; melanoma antigen, family B, 2	1.31	.006 397
Olfr1394	Olfactory receptor 1394	1.3	.029 162
Lrrc16a	Leucine-rich repeat containing 16A	1.3	.046 377
Klf15	Kruppel-like factor 15	1.3	.037 873

Data were analyzed using Affymetrix Transcriptome Analysis Console (Astro-D2KO, n = 4; control, n = 4) at a value of $P < .05$ and a fold change of 1.3 or greater or −1.3 or less in the differential analysis of the microarray data from Cre vs Astro-D2KO hippocampus.

To assess the physiological context of the transcriptional changes that occur in the Astro-D2KO hippocampus, the microarray data were then analyzed by gene ontology to identify gene sets demonstrating enrichment at a nominal < 1%. GSEA revealed three gene sets down-regulated in Astro-D2KO animals (mitochondrial function, ubiquitination, and response to oxidative stress) and three gene sets up-regulated in Astro-D2KO animals (integrin complex, receptor complex, and protein heterodimerization activity) (Table 3).

Given that the Astro-D2KO brain transcriptome was only minimally affected as assessed in the microarray studies, we next used the more sensitive RT-qPCR to measure mRNA levels of candidate genes, starting with known T_3-responsive genes. Accordingly, the expression of four of six positively regulated genes by T_3 were found to be down-regulated in the Astro-D2KO, ie, *Mbp* (~43%), *Mag* (~34%), *Hr* (~49%), and *Aldh1a1* (~61%) (Figure 3N), whereas the expression of 3 of the 12 negatively regulated genes by T_3 were found to be up-regulated in the Astro-D2KO animals, ie, *Dgkg* (~17%), *Syce2* (~26%), and *Col6a1* (~3-fold) (Figure 3N). Next we looked at the expression of genes that are known to be affected in classical animal models of depression. Notably, there was a reduction in the mRNA levels of *Bdnf* (~18%), *Ntf3* (~43%), *Nmdar* (~26%), and *GR* (~20%) (Figure 3N).

Physical exercise rescues phenotype and hippocampal gene expression in Astro-D2KO mice

Regular exercise is known for improving depression and anxiety in rodents (26, 27). To test whether this would also be the case in the Astro-D2KO animals, animals underwent 4 weeks of regular physical activity on a treadmill for 30 minutes. At the end of the exercise period, the animals were tested as before and the differences previously observed between Astro-D2KO and control animals in the OFT (Figure 4, A–F) as well as in the EPM (Figure 4, G–K), TST (Figure 4L), and FST (Figure 4M) were eliminated.

In addition, only 5 days of daily exercises at 60% of S_{max} was sufficient to promote changes in gene expression in the hippocampus (Supplemental Figure 3C) and eliminate the hippocampal differences in mRNA levels between control and Astro-D2KO animals (Figure 4N). Notably, *Vegfa* and *Npas4* mRNA levels decreased in Astro-D2KO animals when compared with controls after exercise (Figure 4N). Unexpectedly, hippocampal *Dio2* mRNA and D2 activity increased by approximately 1.5- and 2.4-fold after daily exercises, respectively (Figure 4, O and P).

Discussion

The present studies reveal that astrocyte-specific *Dio2* inactivation, which does not affect circulating T_3 levels, results in a phenotype of mood dysfunction characterized by depression/anxiety-like behavior and reduced hippocampal expression of *Bdnf*, *Ntf3*, *Nmdar*, and *GR* (Figure 3N), known markers of depression in other animal models. This is likely to stem from changes in hippocampal

Table 2.   Individual Gene Transcripts Up-Regulated in Astro-D2KO Hippocampus

Gene Symbol	Description	Fold	*P* Value
Olfr1357	Olfactory receptor 1357	−1.3	.028 176
Rem2	Rad and gem-related GTP binding protein 2	−1.3	.017 352
Pnldc1	Poly(A)-specific ribonuclease (PARN)-like domain containing 1	−1.3	.016 117
Dennd4c	DENN/MADD domain containing 4C	−1.3	.040 588
Vmn1r9	Vomeronasal 1 receptor 9	−1.3	.009 408
Olfr535	Olfactory receptor 535	−1.3	.013 635
St8sia2	ST8 α-N-acetyl-neuraminide α-2,8-sialyltransferase 2	−1.3	.020 501
Fbxw20	F-box and WD-40 domain protein 20	−1.3	.012 337
Slc23a3	Solute carrier family 23 (nucleobase transporters), member 3	−1.31	.007 156
Mettl24	Methyltransferase like 24	−1.31	.018 338
Mir299a	microRNA 299a	−1.31	.004 738
Dsg4	Desmoglein 4	−1.31	.015 903
Clec4b2	C-type lectin domain family 4, member b2	-−.31	.000 785
Olfr593	Olfactory receptor 593	−1.31	.026 543
Obp1b	Odorant binding protein IB	−1.31	.033 234
Vsig8	V-set and immunoglobulin domain containing 8	−1.32	.002 538
Kremen1	Kringle containing transmembrane protein 1	−1.32	.023 628
Xlr3a	X-linked lymphocyte-regulated 3A	−1.32	.001 963
Lipg	Lipase, endothelial	−1.33	.007 975
Kir3dl1	Killer cell Ig-like receptor, three domains, long cytoplasmic tail, 1	−1.33	.004 548
Dydc2	DPY30 domain containing 2	−1.34	.001 918
Mir1971	microRNA 1971	−1.34	.007 016
Mir376a	microRNA 376a	−1.35	.014 988
Tmem159	Transmembrane protein 159	−1.35	.036 371
Tagap1	T-cell activation GTPase activating protein 1	−1.36	.022 869
Tex26	Testis expressed 26	−1.36	.009 946
Mir153	microRNA 153	−1.38	.000 707
Sprr1b	Small proline-rich protein 1B	−1.39	.002 066
Tas2r136	Taste receptor, type 2, member 136	−1.4	.046 515
Olfr853	Olfactory receptor 853	−1.4	.01 169
Naip6	NLR family, apoptosis inhibitory protein 6; NLR family, apoptosis inhibitory protein 7	−1.43	.047 367
mt-Ts2	Mitochondrially encoded tRNA serine 2	−1.43	.014 508
Mir1955	microRNA 1955	−1.44	.010 293
Olfr591	Olfactory receptor 591	−1.45	.020 531
Olfr811	Olfactory receptor 811	−1.5	.007 783
Orm3	Orosomucoid 3	−1.51	.013 175
Igk-V28	Ig κ-chain variable 28 (V28)	−1.51	.010 163
LOC101055855	Keratin-associated protein 5-5-like	−1.53	.003 359
Tspan18	Tetraspanin 18	−1.54	.031 571
Mir1969	microRNA 1969	−1.56	.016 284
mt-Ts2	Mitochondrially encoded tRNA serine 2; mitochondrially encoded tRNA leucine 2	−1.58	.010 638
Serinc2	Serine incorporator 2	−1.71	.00 931
Gpr115	G protein-coupled receptor 115	−2	.039 619

Data are analyzed as in Table 1.

gene expression that include diminished thyroid hormone signaling (Figure 3N), mitochondrial function, and response to oxidative stress (Table 3). Gene set analyses also indicate enrichment in genes related to immune response and inflammation (Table 3). Remarkably, daily sessions of treadmill exercise eliminated the anxiety-depression-like Astro-D2KO phenotype (Figure 4, A–M) as well as differences in hippocampal expression of depression markers (Figure 4N). In addition, physical exercise also normalized the expression of the T_3-responsive genes in the Astro-D2KO hippocampus (Figure 4N). Given that greater than 90% of brain Dio2 was inactivated in the Astro-D2KO animals, it is conceivable that the normalization of gene

expression by physical exercise indicates that nonthyroid-related stimuli can influence the expression T_3-responsive genes.

Depression-anxiety-like behavior is typically seen in systemically hypothyroid mice and in humans (28); it has also been reported in TR-α1 knockout mice (22, 29, 30). In all cases this is the result of decreased thyroid hormone action in the brain. Here we defined that brain hypothyroidism resulting from astrocyte-specific *Dio2* disruption is also associated with depressive behavior. This was first suspected in the analysis of 24-hour ambulatory profiles later confirmed by standard tests such as the TST (Figure 3L) and FST (Figure 3M). In addition, results obtained in

Table 3. Gene Ontology Sets Enriched in the Comparison of Expression Data Between Cre Versus Astro-D2KO Hippocampus Samples

Gene Ontology	Description	Genes Enriched in Our Samples, n	Total Genes in Set, n	ES	NES	Nominal P Value
n	Down-regulated in Astro-D2KO					
0015078	Hydrogen ion transmembrane transporter activity	11	25	0.51	1.58	<.01
0016881	Acid amino acid ligase activity	20	54	0.33	1.55	<.01
0006979	Response to oxidative stress	12	41	0.35	1.4	<.01
n	Up-regulated in Astro-D2KO					
0008305	Integrin complex	9	18	−0.69	−1.58	<.01
0043235	Receptor complex	22	53	−0.63	−1.53	<.01
0046982	Protein heterodimerization activity	16	73	−0.45	−1.53	<.01

Abbreviations: ES, enrichment score; NES, normalize enrichment score. All gene sets were significantly enriched or impoverished at a nominal value of $P < 1$.

the EPM (Figure 3, G–K) revealed anxiety-like behavior, with the Astro-D2KO animals spending more time in the closed arms of the maze (Figure 3I), more freezing time (Figure 3J), and less head dips (Figure 3K). Notably, the OFT (Figure 3, A–F) revealed no indication of increased emotionality, which could be explained by differences in its emotional context: the OFT was performed under low luminosity, which triggers exploration of the new environment. In contrast, the EPM is a test with high emotionality, which normally triggers an underlining anxiety behavior.

Reduced locomotor activity is a known confounder in interpreting behavioral tests of anxiety-like and depressive-like behavior. For example, reduced entries into open arms, reduced struggling, or reduced swimming might be explained just by reduced locomotor activity. However, the data indicate otherwise: the reduction in ambulatory movements of the Astro-D2KO animals was selective, ie, only in the Y but not the X component (Figure 2, A–H); in addition, the Astro-D2KO animals performed similarly as the control animals in the following: 1) the S_{max} and the 5-day treadmill sessions (Supplemental Figure 3B); 2) the total number of entries in the open arms of the EPM (the reduction in the number of entries in the closed arms is because the residence time inside the closed arms was longer; Supplemental Figure 2E-F); and 3) in the 48-hour accumulated number of revolutions in the free-running wheel (Supplemental Figure 3A). All of these factors suggest the unlikelihood that the reduced locomotor activity in Astro-D2KO animals, as assessed through ambulatory movement in the CLAMS (Figure 2), influenced the be-

haviors observed in the formal tests of anxiety-like and depressive-like behavior (Figure 3).

In other mouse models of brain hypothyroidism, the mechanism leading to depression seems to involve decreased T_3 signaling in the hippocampus, which reportedly leads to impaired neurogenesis (31). Even though neurogenesis was unaffected in the Astro-D2KO hippocampus (Figure 1M), the altered expression of T_3-responsive genes (Figure 3N) supports diminished thyroid hormone signaling after *Dio2* disruption. This explains the present findings of depression/anxiety-like behavior in the Astro-D2KO.

Overall, the changes in gene expression observed in the Astro-D2KO hippocampus were not dramatic. The reduction in mitochondrial genes observed in the GSEA of Astro-D2KO hippocampus is reminiscent of the well-known metabolic effects of T_3, which could also justify the decreased expression in genes involved in response to oxidative stress (Table 3). An unexpected finding, however, was the observation of multiple genes related to inflammation and immune response in the three gene sets enriched in the Astro-D2KO hippocampus (Table 3). It is unclear at the moment how dampening thyroid hormone signaling in the hippocampus results in such changes in transcriptome. Nonetheless, it is well known that central nervous system (CNS) inflammation underlies depression models (32), which could be a contributing factor in the depression-anxiety-like behavior observed in the Astro-D2KO mouse.

It is remarkable that repeated exercise sessions eliminated the mood dysfunction (depression/anxiety-like be-
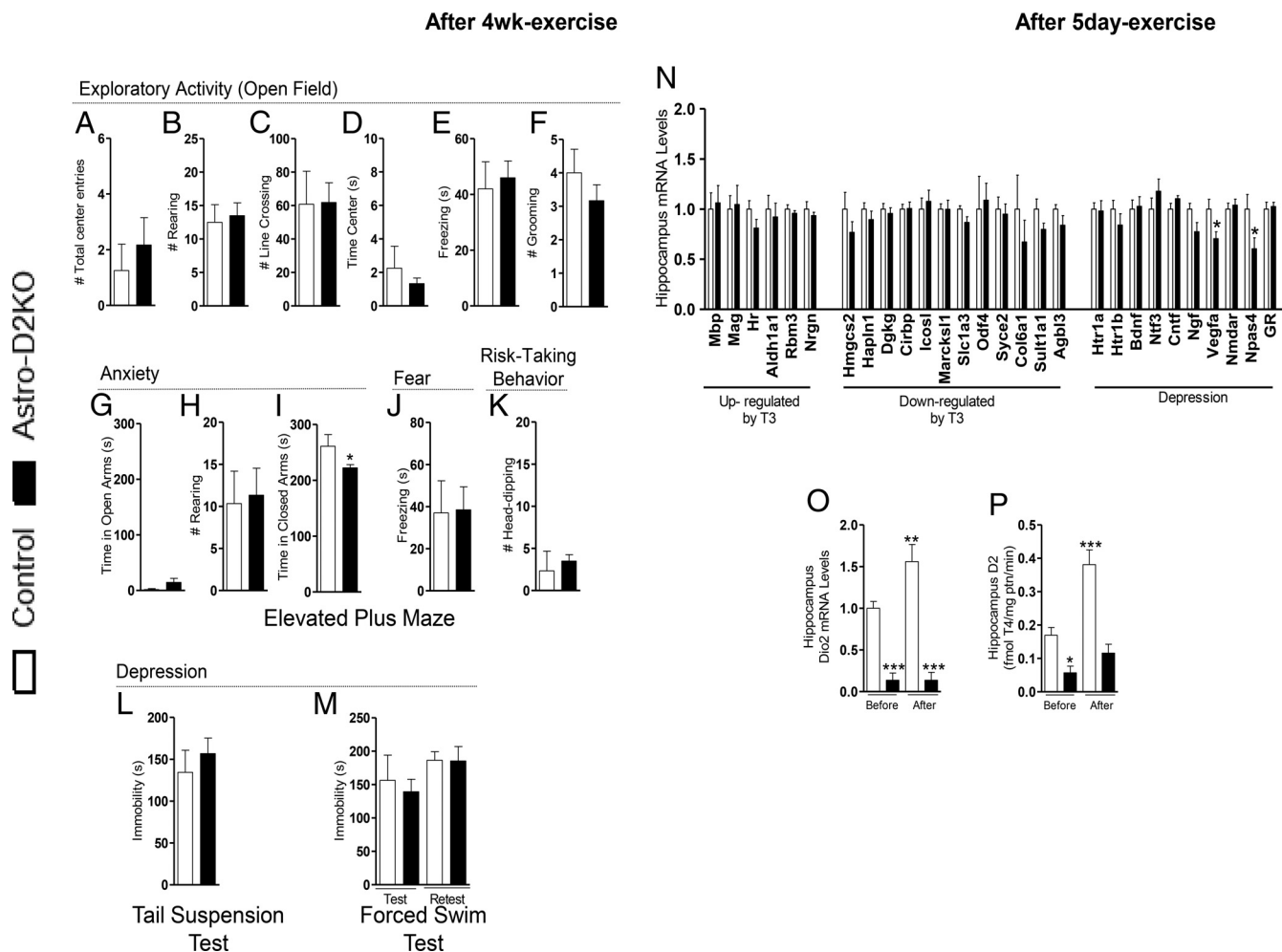
Figure 4. Behavior phenotype and hippocampal gene profile in Astro-D2KO mice after treadmill exercise. A–M, Behavioral tests after 4 weeks of running exercise on treadmill. A–F, OFT. A, Total number of center entries. B, Total number of rearing. C, Total number of line crossing. D, Total time in center. E, Total time of freezing. F, Total number of grooming. G–K, EPM. G, Time spent in open arms. H, Total number of rearing. I, Time spent in closed arms. J, Total time of freezing. K, Total number of head-dips. L, TST, time of immobility. M, FST, time of immobility. N–P, Astro-D2KO after treadmill exercise for 5 days. N, mRNA levels of T3 responsive genes and genes related to depression in hippocampus. O, *Dio2* mRNA levels in hippocampus, before and after exercise, measured by RT-qPCR and using CycloA as the internal control. P, D2 activity in hippocampus, before and after exercise. Values are the mean ± SEM (n = 3–6). *, $P < .05$, ***, $P < .001$ compared with control mice.

havior) and alterations in hippocampal gene expression (Figure 4N). In fact, treadmill exercise ameliorates symptoms of hypothyroidism through enhanced neurogenesis (33). In the case of depression, the efficacy of exercise is well known, and it has been classically attributed to changes in neurotransmitter metabolism, neurotrophic factors, and/or neuroinflammation (34–37). Along these lines, it is notable that *Dio2* expression in the hippocampus increases with exercise sessions in the control animals (Figure 4, O and P), whereas the serum T_3 and T_4 levels remained stable (23); this could theoretically be an adjuvant mechanism through which exercise improves depression. However, exercise was very effective in correcting depression in the Astro-D2KO animals, suggesting that *Dio2* activation probably plays only a minor role if any in this process.

Absence of D2-mediated T_3 production in different development organs underlies permanent defects that are carried through adulthood such as in the inner ear (38), brown adipose tissue (39), and liver (40). Given that the developing brain also expresses *Dio2*, a major CNS phenotype in the Astro-D2KO animals would be expected, especially given that congenital hypothyroidism in animal models and humans is associated with brain structural abnormality (41), diminished number of cells in granular layers of the hippocampus and cerebellum (41), and delayed/poor myelinization (42, 43). Thus, it is indeed notable that the global-D2KO mouse lacks a major CNS phenotype, exhibiting only agility impairment (7), and the Astro-D2KO exhibits a reversible mood dysfunction phenotype (Figure 4, A–M). In fact, Astro-D2KO animals exhibit normal morphology as seen in the hippocampus,

Table 4. Antibody Table

Target	Name	Manufacturer, Catalog Number	Species Raised (Monoclonal, Polyclonal), Dilution
Human MBP	Anti-MBP	Merck-Millipore, AB980	Rabbit polyclonal, 1:250
BrdU	Anti-BrdU	Abcam, Ab1893	Sheep polyclonal, 1:300
Human HuC/HuD	Anti HuC + HuD neuronal protein Antibody, biotin conjugate	Life Technologies/ThermoFisher Scientific A-21272	Mouse monoclonal, 1:300

dentate gyrus, cerebellum, and cerebral cortex (Figure 1, I—L and P–U). Neurogenesis is unaffected in the dentate gyrus (Figure 1M), and myelin density in the hippocampus and corpus callosum is normal (Figure 1, N–O, and V–Y). Thus, it is conceivable that the early D2 inactivation in the global-D2KO or Astro-D2KO animals sets off compensatory mechanisms that obviate the role played by D2 in the adult CNS.

Previous studies suggest that deiodination in the brain might play a role in mood disorders. For example, administration of antidepressants increases D2 activity in the rodent brain (44, 45). At the same time, a mouse that is resistant to stress-induced depression exhibits increased hippocampal expression of *Dio2* and *Dio3* (46). In contrast, a mouse with global inactivation of *Dio3* exhibits aggressive behavior and indifference toward pups due to brain thyrotoxicosis (14). Clinical studies are unfortunately limited to patients with hypo- or hyperthyroidism, with the former exhibiting variable degrees of cognitive dysfunction, depression, and mood disorders (47). Indeed, the use of magnetic resonance imaging spectroscopy and positron emission tomography has confirmed that thyroid hormones act in the human limbic system (48); they also potentiate the efficacy of antidepressant agents when given to euthyroid individuals (49). A potential clinical role played by deiodinases is much less clear. Whereas mutations that interfere with the D2 pathway have not been identified, a prevalent single-nucleotide polymorphism in the *Dio2* gene (Thr92AlaD2) that is present in 12%–36% of individuals in the general population has been associated with mental and psychological disorders, such as mental retardation, bipolar disorder, and low intelligence quotient (47). The Thr92AlaD2 polymorphism is also associated with a preference for levothyroxine plus liothyronine combination therapy vs levothyroxine monotherapy among carriers with hypothyroidism (50). In summary, studies in mice with astrocyte-specific *Dio2* inactivation suggest a role played by D2 in thyroid hormone signaling in the brain, the disruption of which leads to a mood/behavior phenotype. The data highlight that potential defects in the D2 pathway might have clinical relevance; possibly constituting a risk factor for mood or behavioral disorders. The finding that physical exercise reverts the Astro-D2KO phenotype is exciting, opening the fascinating possibility that physical exercise could be used to improve mood disorders in hypothyroid patients.

Appendix

See Table 4.

Acknowledgments

Address all correspondence and requests for reprints to: Antonio C. Bianco, MD, PhD, Division of Endocrinology and Metabolism, Rush University Medical Center, 1735 West Harrison Street, Chicago, IL 60612. E-mail: abianco@deiodinase.org; or Miriam O. Ribeiro, PhD, Developmental Disorders Program, Center of Biological Science and Health, Mackenzie Presbiteryan University, Rua da Consolação, 930, São Paulo SP 01302-900 Brazil. E-mail: miriamribeiro@mackenzie.br.

References

1. **Visser WE, Friesema EC, Visser TJ.** Thyroid hormone transporters: the knowns and the unknowns. *Mol Endocrinol*. 2011;25:1–14.
2. **Callebaut I, Curcio-Morelli C, Mornon JP, et al.** The iodothyronine selenodeiodinases are thioredoxin-fold family proteins containing a glycoside hydrolase clan GH-A-like structure. *J Biol Chem*. 2003; 278:36887–36896.
3. **Curcio-Morelli C, Gereben B, Zavacki AM, et al.** In vivo dimeriza-

tion of types 1, 2, and 3 iodothyronine selenodeiodinases. *Endocrinology*. 2003;144:937–946.

4. **Freitas BC, Gereben B, Castillo M, et al.** Paracrine signaling by glial cell-derived triiodothyronine activates neuronal gene expression in the rodent brain and human cells. *J Clin Invest*. 2010;120:2206–2217.

5. **Crantz FR, Silva JE, Larsen PR.** An analysis of the sources and quantity of 3,5,3′-triiodothyronine specifically bound to nuclear receptors in rat cerebral cortex and cerebellum. *Endocrinology*. 1982; 110:367–375.

6. **Crantz FR, Larsen PR.** Rapid thyroxine to 3,5,3′-triiodothyronine conversion and nuclear 3,5,3′-triiodothyronine binding in rat cerebral cortex and cerebellum. *J Clin Invest*. 1980;65:935–938.

7. **Galton VA, Wood ET, St Germain EA, et al.** Thyroid hormone homeostasis and action in the type 2 deiodinase-deficient rodent brain during development. *Endocrinology*. 2007;148:3080–3088.

8. **Galton VA, Schneider MJ, Clark AS, Germain DLS.** Life without thyroxine to 3,5,3′-triiodothyronine conversion: studies in mice devoid of the 5′-deiodinases. *Endocrinology*. 2009;150:2957–2963.

9. **Morte B, Ceballos A, Diez D, et al.** Thyroid hormone-regulated mouse cerebral cortex genes are differentially dependent on the source of the hormone: a study in monocarboxylate transporter-8- and deiodinase-2-deficient mice. *Endocrinology*. 2010;151:2381–2387.

10. **Galton VA, de Waard E, Parlow AF, St Germain DL, Hernandez A.** Life without the iodothyronine deiodinases. *Endocrinology*. 2014; 155:4081–4087.

11. **Baqui M, Botero D, Gereben B, et al.** Human type 3 iodothyronine selenodeiodinase is located in the plasma membrane and undergoes rapid internalization to endosomes. *J Biol Chem*. 2003;278:1206–1211.

12. **Kallo I, Mohacsik P, Vida B, et al.** A novel pathway regulates thyroid hormone availability in rat and human hypothalamic neurosecretory neurons. *PLoS One*. 2012;7:e37860.

13. **Jo S, Kallo I, Bardoczi Z, et al.** Neuronal hypoxia induces hsp40-mediated nuclear import of type 3 deiodinase as an adaptive mechanism to reduce cellular metabolism. *J Neurosci*. 2012;32:8491–8500.

14. **Hernandez A, Martinez ME, Fiering S, Galton VA, St Germain D.** Type 3 deiodinase is critical for the maturation and function of the thyroid axis. *J Clin Invest*. 2006;116:476–484.

15. **Bianco AC, Salvatore D, Gereben B, Berry MJ, Larsen PR.** Biochemistry, cellular and molecular biology, and physiological roles of the iodothyronine selenodeiodinases. *Endocr Rev*. 2002;23:38–89.

16. **Silva JE, Larsen PR.** Regulation of thyroid hormone expression at the prereceptor and receptor levels. In: Hennemann G, ed. *Thyroid Hormone Metabolism*. 1st ed. New York and Basel: Marcel Dekker, Inc; 1986:441–500.

17. **Peeters R, Fekete C, Goncalves C, et al.** Regional physiological adaptation of the central nervous system deiodinases to iodine deficiency. *Am J Physiol Endocrinol Metab*. 2001;281:E54–E61.

18. **Fonseca TL, Correa-Medina M, Campos MP, et al.** Coordination of hypothalamic and pituitary T3 production regulates TSH expression. *J Clin Invest*. 2013;123:1492–1500.

19. **Fonseca TL, Werneck-De-Castro JP, Castillo M, et al.** Tissue-specific inactivation of type II deiodinase reveals multi-level control of fatty acid oxidation by thyroid hormone in the mouse. *Diabetes* 2014;63(5):1594–1604.

20. **Bianco AC, Anderson G, Forrest D, et al.** American Thyroid Association guide to investigating thyroid hormone economy and action in rodent and cell models. *Thyroid*. 2014;24:88–168.

21. **Hunsberger J, Duman C.** Animal models for depression-like and anxiety-like behavior. *Protocol Exchange*. 2007;1–4. http://www.nature.com/protocolexchange/protocols/344

22. **Venero C, Guadano-Ferraz A, Herrero AI, et al.** Anxiety, memory impairment, and locomotor dysfunction caused by a mutant thyroid

hormone receptor alpha1 can be ameliorated by T3 treatment. *Genes Dev*. 2005;19:2152–2163.

23. **Bocco BM, Louzada RA, Silvestre DH, et al.** Thyroid hormone activation by type-2 deiodinase mediates exercise-induced PGC-1a expression in skeletal muscle. *J Physiol*. In press.

24. **Werneck-de-Castro JP, Fonseca TL, Ignacio DL, et al.** Thyroid hormone signaling in male mouse skeletal muscle is largely independent of D2 in myocytes. *Endocrinology*. 2015;156:3842–3852.

25. **Castillo M, Hall JA, Correa-Medina M, et al.** Disruption of thyroid hormone activation in type 2 deiodinase knockout mice causes obesity with glucose intolerance and liver steatosis only at thermoneutrality. *Diabetes*. 2011;60:1082–1089.

26. **Hong YP, Lee HC, Kim HT.** Treadmill exercise after social isolation increases the levels of NGF, BDNF, and synapsin I to induce survival of neurons in the hippocampus, and improves depression-like behavior. *J Exerc Nutrition Biochem*. 2015;19:11–18.

27. **Kim TW, Lim BV, Baek D, Ryu DS, Seo JH.** Stress-induced depression is alleviated by aerobic exercise through up-regulation of 5-hydroxytryptamine 1A receptors in rats. *Int Neurourol J*. 2015;19: 27–33.

28. **Ittermann T, Volzke H, Baumeister SE, Appel K, Grabe HJ.** Diagnosed thyroid disorders are associated with depression and anxiety. *Soc Psychiatry Psychiatr Epidemiol*. 2015;50:1417–1425.

29. **Guadano-Ferraz A, Benavides-Piccione R, Venero C, et al.** Lack of thyroid hormone receptor α1 is associated with selective alterations in behavior and hippocampal circuits. *Mol Psychiatry*. 2003;8:30–38.

30. **Buras A, Battle L, Landers E, Nguyen T, Vasudevan N.** Thyroid hormones regulate anxiety in the male mouse. *Horm Behav*. 2014; 65:88–96.

31. **Montero-Pedrazuela A, Venero C, Lavado-Autric R, et al.** Modulation of adult hippocampal neurogenesis by thyroid hormones: implications in depressive-like behavior. *Mol Psychiatry*. 2006;11: 361–371.

32. **Felger JC, Lotrich FE.** Inflammatory cytokines in depression: neurobiological mechanisms and therapeutic implications. *Neuroscience*. 2013;246:199–229.

33. **Shin MS, Ko IG, Kim SE, et al.** Treadmill exercise ameliorates symptoms of methimazole-induced hypothyroidism through enhancing neurogenesis and suppressing apoptosis in the hippocampus of rat pups. *Int J Dev Neurosci*. 2013;31:214–223.

34. **Kohut ML, McCann DA, Russell DW, et al.** Aerobic exercise, but not flexibility/resistance exercise, reduces serum IL-18, CRP, and IL-6 independent of β-blockers, BMI, and psychosocial factors in older adults. *Brain Behav Immun*. 2006;20:201–209.

35. **Nabkasorn C, Miyai N, Sootmongkol A, et al.** Effects of physical exercise on depression, neuroendocrine stress hormones and physiological fitness in adolescent females with depressive symptoms. *Eur J Public Health*. 2006;16:179–184.

36. **Van der Borght K, Kobor-Nyakas DE, Klauke K, et al.** Physical exercise leads to rapid adaptations in hippocampal vasculature: temporal dynamics and relationship to cell proliferation and neurogenesis. *Hippocampus*. 2009;19:928–936.

37. **Sousa e Silva T, Longui CA, Rocha MN, et al.** Prolonged physical training decreases mRNA levels of glucocorticoid receptor and inflammatory genes. *Horm Res Paediatr*. 2010;74:6–14.

38. **Ng L, Goodyear RJ, Woods CA, et al.** Hearing loss and retarded cochlear development in mice lacking type 2 iodothyronine deiodinase. *Proc Natl Acad Sci USA*. 2004;101:3474–3479.

39. **Hall JA, Ribich S, Christoffolete MA, et al.** Absence of thyroid hormone activation during development underlies a permanent defect in adaptive thermogenesis. *Endocrinology*. 2010;151:4573–4582.

40. **Fonseca TL, Fernandes GW, McAninch EA, et al.** Perinatal deiodinase 2 expression in hepatocytes defines epigenetic susceptibility to liver steatosis and obesity. *Proc Natl Acad Sci USA*. 2015;112: 14018–14023.

41. **Madeira MD, Paula-Barbosa M, Cadete-Leite A, Tavares MA.** Un-

biased estimate of hippocampal granule cell numbers in hypothyroid and in sex-age-matched control rats. *J Hirnforsch*. 1988;29:643–650.

42. **Malone MJ, Rosman NP, Szoke M, Davis D.** Myelination of brain in experimental hypothyroidism. An electron-microscopic and biochemical study of purified myelin isolates. *J Neurol Sci*. 1975;26:1–11.

43. **Noguchi T, Sugisaki T.** Hypomyelination in the cerebrum of the congenitally hypothyroid mouse (hyt). *J Neurochem*. 1984;42:891–893.

44. **Campos-Barros A, Meinhold H, Stula M, et al.** The influence of desipramine on thyroid hormone metabolism in rat brain. *J Pharmacol Exp Ther*. 1994;268:1143–1152.

45. **Baumgartner A, Dubeyko M, Campos-Barros A, Eravci M, Meinhold H.** Subchronic administration of fluoxetine to rats affects triiodothyronine production and deiodination in regions of the cortex and in the limbic forebrain. *Brain Res*. 1994;635:68–74.

46. **Markova N, Chernopiatko A, Schroeter CA, et al.** Hippocampal gene expression of deiodinases 2 and 3 and effects of 3,5-diiodo-L-thyronine T2 in mouse depression paradigms. *Biomed Res Int*. 2013;2013:565218.

47. **Gereben B, McAninch EA, Ribeiro MO, Bianco AC.** Scope and limitations of iodothyronine deiodinases in hypothyroidism. *Nat Rev Endocrinol*. 2015;11:642–652.

48. **Zhang Q, Bai Z, Gong Y, et al.** Monitoring glutamate levels in the posterior cingulate cortex of thyroid dysfunction patients with TE-averaged PRESS at 3T. *Magn Reson Imaging*. 2015;33:774–778.

49. **Almeida OP, Alfonso H, Flicker L, Hankey G, Chubb SA, Yeap BB.** Thyroid hormones and depression: the Health in Men study. *Am J Geriatr Psychiatry*. 2011;19:763–770.

50. **Panicker V, Saravanan P, Vaidya B, et al.** Common variation in the DIO2 gene predicts baseline psychological well-being and response to combination thyroxine plus triiodothyronine therapy in hypothyroid patients. *J Clin Endocrinol Metab*. 2009;94:1623–1629.